Accepted Manuscript

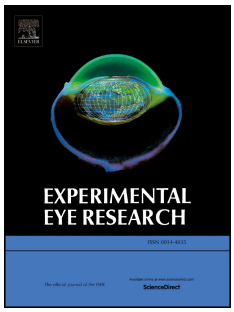

Novel anti-inflammatory liposomal formulation for the pre-ocular tear film: *In vitro* and *ex vivo* functionality studies in corneal epithelial cells

Laura Soriano-Romaní, Marta Vicario-de-la-Torre, Mario Crespo-Moral, Antonio López-García, Rocío Herrero-Vanrell, Irene T. Molina-Martínez, Yolanda Diebold

PII: S0014-4835(16)30450-X

DOI: 10.1016/j.exer.2016.11.010

Reference: YEXER 7058

To appear in: *Experimental Eye Research*

Received Date: 28 June 2016

Revised Date: 7 October 2016

Accepted Date: 9 November 2016

Please cite this article as: Soriano-Romaní, L., Vicario-de-la-Torre, M., Crespo-Moral, M., López-García, A., Herrero-Vanrell, R., Molina-Martínez, I.T., Diebold, Y., Novel anti-inflammatory liposomal formulation for the pre-ocular tear film: *In vitro* and *ex vivo* functionality studies in corneal epithelial cells, *Experimental Eye Research* (2016), doi: 10.1016/j.exer.2016.11.010.

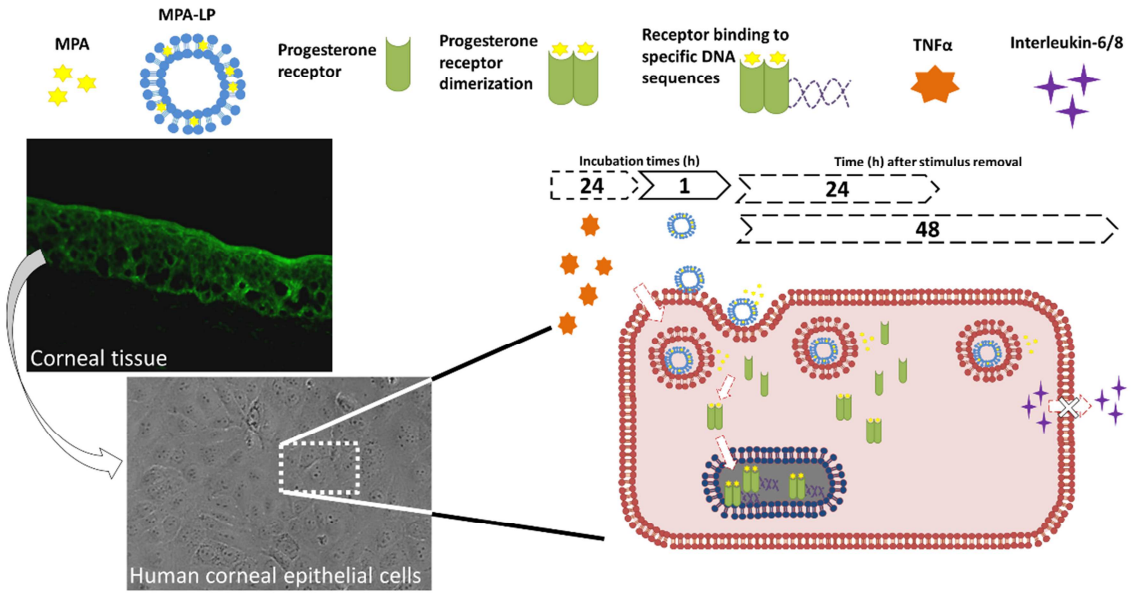

Title

Novel anti-inflammatory liposomal formulation for the pre-ocular tear film: *in vitro* and *ex vivo* functionality studies in corneal epithelial cells

Author names and affiliations

Laura Soriano-Romaní,[1,2*] Marta Vicario-de-la-Torre,[3*] Mario Crespo-Moral,[1] Antonio López-García,[1,2] Rocío Herrero-Vanrell,[3] Irene T. Molina-Martínez,[3] and Yolanda Diebold[1,2]

[1]Ocular Surface Group, IOBA - University of Valladolid, Valladolid, Spain

[2]Biomedical Research Networking Center on Bioengineering, Biomaterials and Nanomedicine (CIBER-BBN), Spain

[3]Department of Pharmacy and Pharmaceutical Technology, School of Pharmacy, Complutense University of Madrid, Madrid, Spain

*These authors contributed equally to the work.

Corresponding author(s)

Yolanda Diebold, PhD

Ocular Surface Group, IOBA - University of Valladolid

Edificio IOBA, Campus Miguel Delibes, Paseo de Belén 17. 47011 Valladolid, Spain

Phone: +34-983-18 47 50; Fax: +34-983-18 47 62

Email: yol@ioba.med.uva.es

Irene Molina Martínez, PhD

Department of Pharmacy and Pharmaceutical Technology, School of Pharmacy, Complutense University of Madrid

Plaza Ramón y Cajal s/n. 28040, Madrid, Spain

Phone: +34913941739; Fax: +34913941736

Email: iremm@ucm.es

Abstract

In ocular surface inflammatory diseases, such as dry eye disease, long-term symptom relief requires targeting the inflammation itself rather than treating only the surface-associated dryness with artificial tears. Therefore, we included an anti-inflammatory agent in an unpreserved liposome-based (LP) formulation used as artificial tears. Our aim was to characterize and study its *in vitro* and *ex vivo* cell uptake and functionality. Human corneal epithelial (HCE) cells were used to study MPA-LP-induced effects after 60 min of exposure, using blank LP and non-LP MPA formulations as controls. A fluorescent labeled LP formulation was used to determine uptake by HCE cells and localization in *ex vivo* porcine corneas. The LP formulation complied with the required physicochemical properties and had no cytotoxicity on HCE cells after 60 min of exposure. HCE cells showed LP-associated fluorescence at 24, 48, and 72 h after 60 min of exposure, and the LP-associated fluorescence was uniformly distributed throughout the porcine corneal epithelium immediately after 5 min of exposure. MPA-LP increased protein expression and nuclear translocation of progesterone receptor in comparison with controls as determined by Western blotting and immunofluorescence. Moreover, MPA-LP significantly reduced the cell proliferation rate and IL-6 and IL-8 production 48 h after the exposure period, as determined by the alamarBlue assay and ELISA, respectively. None of these effects were evident in blank LP-exposed cells and non-LP MPA formulation reduced only IL-6 production. Our results suggest that the LP-based formulation, used to replenish the lipids of the tear film, can be loaded with anti-inflammatory agents that can be delivered into the cells and activate specific drug receptors. These agents can reduce inflammatory cytokine production and may be effective in the treatment of inflammatory processes associated with ocular surface diseases.

Keywords

Corneal epithelial cells; drug delivery; glucocorticoid receptor; inflammation; liposome; progesterone receptor.

Abbreviations

BAC: benzalkonium chloride

C6: coumarin-6

DED: dry eye disease

DMEM/F12: Dulbecco's Modified Eagle Medium + F12 medium mixture

EE: encapsulation efficiency

ELISA: enzyme-linked immunosorbent assay

GAPDH: glyceraldehyde 3-phosphate dehydrogenase

HCE: human corneal epithelial

HPLC: high performance liquid chromatography

IL: interleukin

LP: liposome

MPA: medroxyprogesterone acetate

PBS: phosphate buffered saline

PC: phosphatidylcholine

SEM: standard error of the mean

TNFα: tumor necrosis factor-alpha

XTT: 2,3-bis-(2-methoxy-4-nitro-5-sulfophenyl)-2H-tetrazolium-5-carboxanilide

1. Introduction

Eye tissues are affected by diverse inflammation-based diseases that can be devastating as eyesight is impaired. A paradigm of such inflammatory disorders is dry eye disease (DED), a common age-related ocular pathology that results from dysfunction of the ocular surface and/or tissues that produce the tears. The primary effects of patients with DED are impaired functional visual acuity and low quality of life. At the molecular level, the main reason of these effects is an underlying inflammation process that profoundly alters the ocular surface tissues and the tear film. Recent research has led to innovations in the pharmacological treatment of DED. These advances have focused on tear replacement or tear preservation with novel artificial tears, topical and systemic anti-inflammatory and immunosuppressive therapy, and even the use of medical devices in the more severe grades of the disease (Pflugfelder et al. 2000). Despite significant progress in these treatments, the disease in many patients is not fully alleviated. Although current treatments with artificial tears are the first step for symptomatic relief, the ongoing inflammation is not addressed. The use of drug delivery systems is of great interest to improve the pharmacological management of DED because they can encapsulate active agents, direct them to the target tissue/cells, and release the cargo in a controlled fashion (Diebold and Calonge. 2010, Patel et al. 2013). In topically administered drugs, these devices overcome drawbacks such as low bioavailability due to the tear film barrier, rapid drainage, and poor corneal permeation.

Among drug delivery systems, liposomes (LPs), which are vesicles containing an aqueous core and delimited by a membrane-like lipid bilayer, ensure good biological compatibility and reduced toxicity. The existence of an aqueous core and the lipid bilayer confers the ability to encapsulate both hydrophilic and lipophilic compounds with improved drug stability. LPs have been employed to improve drug transport across the cornea (Di Tommaso et al. 2012) with prolonged drug effect (Hathout et al. 2007, Law et al. 2000). The idea of using LPs as carriers for topically administered anti-inflammatory drugs was first reported in 1982 (Schaeffer and Krohn. 1982) and has been continuously revised (Lim et al. 2015). Corticosteroids are potent anti-inflammatory agents, poorly soluble in aqueous solution, which makes them good candidates for being encapsulated in drug delivery systems. However, with prolonged treatment, the potent activity of these drugs often causes adverse effects, such as increased intraocular pressure or cataract formation. For this reason, synthetic “soft”

anti-inflammatory steroids, like medroxyprogesterone acetate (MPA), are frequently prescribed for topical administration in the eye.

Taking all of this information into account, our aim was to prepare and characterize a LP-based formulation loaded with the anti-inflammatory agent MPA that could be used as topically instilled artificial tears. Prior to proceeding with *in vivo* studies, it was necessary to determine by *in vitro* studies how corneal epithelial cells take up the drug delivery system and the encapsulated drug. Then, we asked whether or not the encapsulated drug was delivered into the cells and activated glucocorticoid and progesterone receptors, eliciting an anti-inflammatory effect in an *in vitro* inflammation model of human corneal epithelial cells.

2. Materials and methods

2.1. Materials and equipment

All materials used in this study were purchased from Sigma-Aldrich (St. Louis, MO) except as follows: Phospholipon 90G, >95% of phosphatidylcholine (PC), was purchased from Lipoid GmbH (Cologne, Germany) and trehalose was acquired from Cymit Química S.L. (Barcelona, Spain). The MPA-commercial, non-LP formulation or reference formulation Colircusi Medrivas® was from Alcon Cusi S.A. (Barcelona, Spain). Dulbecco's Modified Eagle Medium (DMEM)/F12 and some of its supplements, such as fetal bovine serum, penicillin, and streptomycin were from Invitrogen-GIBCO (Inchinnan, UK). Human epidermal growth factor and bovine insulin were from Invitrogen (Eugene, OR). Cell culture plates and multichamber Permanox® or Glass® slides were from Nunc (Roskilde, Denmark). For Western blot experiments, the bicinchoninic acid assay was from Pierce (Rockford, IL) and acrylamide and Tris-buffered saline were purchased from Bio-Rad Laboratories (Hercules, CA). For immunocytochemistry and Western blotting, mouse monoclonal primary antibodies for glucocorticoid and progesterone receptors were from Abcam (Cambridge, UK), and the antibody for glyceraldehyde 3-phosphate dehydrogenase (GAPDH) was from Santa Cruz Biotechnology (Santa Cruz, CA). Fluoromount-G™ mounting media was from SouthernBiotech (Birmingham, AL). The alamarBlue® colorimetric indicator assay was from AbD Serotec (Oxford, UK). Tumor necrosis factor alpha (TNFα) was from PeproTech (London, UK). Human interleukin-6 (IL-6) and IL-8 enzyme-linked immunosorbent assay (ELISA) kits were from Diaclone (Bensançon, France). The

Lipex Extruder® was from Lipex Biomembrane™ (Vancouver, Canada) and the particle size analyzer Zetatrac® was from Microtrac-Europe GmbH (Meerbusch, Germany). The high performance liquid chromatography (HPLC) Waters 600 E, binary HPLC pump, 717 Plus autosampler, in-line degasser, and 486 λ absorbance detector was from Waters (Barcelona, Spain) and the Mediterranean Sea® C18 100 Å 5-µm column (150 mm by 4 mm) from Teknokroma, S.A. (Barcelona, Spain). The osmometer K-7000 was from Knauer (Berlin, Germany) and the thermostatically controlled rheometer Rheostress RS1 was from Haake Technik GmbH (Düsseldorf, Germany). The SpectraMAX® M5 multidetection microplate reader and the SoftMax Pro 4.8 software used for absorbance and fluorescence measurements were from Molecular Devices (Sunnyvale, CA). The Leica DMI 6000B microscope and the LAS AF Lite software and ImageJ software v. 1.49 (http://imagej.nih.gov/ij/) used to visualize and analyze fluorescence micrographs, were from Leica Microsystems (Wetzlar, Germany) and from National Institutes of Health (Bethesda, MD), respectively. Final fluorescence micrographs were minimally adjusted in terms of brightness and contrast using Adobe Photoshop version 8.0.1. The ChemiDoc XRS system and the Quantity One software used to visualize the acrylamide gel and to analyze the resulting images were from Bio-Rad Laboratories. The IBM SPSS Statistics version 23.0 software used for statistical analyses was from IBM Corp. (Armonk, NY).

2.2. Liposomal formulation preparation and fluorescent labeling

LP formulation composed of PC, cholesterol, vitamin E, and MPA at a molar ratio 13:3:0.2:0.3 was prepared by the solvent evaporation technique as previously described (Vicario-de-la-Torre et al. 2014). The film formed was hydrated with a dispersion solution comprised of borate buffer solution (135.5 mM) containing trehalose (42.5 mM). The MPA-LP formulations were extruded through a size-controlled 0.22-µm pore size polycarbonate membrane for ten cycles under nitrogen pressure (≤200 psi) to obtain lipid vesicles with a unimodal size distribution. Final PC and MPA concentrations in the resultant dispersion were 20 mg/mL and 200 µg/mL, respectively.

To obtain fluorescently-labeled LP formulation, the lipid mixture containing coumarin-6 (C6) instead of MPA was dissolved in chloroform, and the C6-LP formulation was obtained following the protocol described above. Fluorescent C6-LP at a final C6 concentration of 20 µg/mL was used in human corneal epithelial (HCE) cells

and *ex vivo* porcine corneas (see sub-section 2.6 below). To determine LP-associated fluorescence, a suspension of C6 (not in liposomes) obtained from the supernatant after C6-LP centrifugation (49,263 g for 60 min at 10ºC) was used as the control.

2.3. Characterization of liposomal formulation

2.3.1. Particle size distribution and encapsulation efficiency

Particle size distribution of blank, MPA-, and C6-LP formulations were measured by dynamic light scattering using a particle size analyzer at room temperature.

To determine the encapsulation efficiency, the LP formulation was centrifuged (49,263 g for 60 min at 10ºC), and the supernatant was then analyzed by HPLC at 40ºC. Isocratic MPA analysis was performed with a mobile phase of acetonitrile/tetrahydrofurane/ultrapure milliQ water (45/10/45), a flow rate of 1 mL min^{-1}, and detection at 254 nm. The retention time was 12.5 min. This analytical procedure, described in Pharmacopeia (Shabir. 2003), was previously validated in our laboratory with regard to linearity, precision, and accuracy parameters. Encapsulation efficiency (*EE*) was calculated as follows:

$$EE = \frac{C0 - C1}{C0} * 100$$

Where *C0* and *C1* were the concentration of the drug in the LP dispersion and in the supernatant after centrifugation.

2.3.2. pH, osmolarity, and viscosity measurements

The pH of the MPA- and C6-LP formulations was measured using a pH meter in triplicate at room temperature.

Osmolarity was analyzed by a vapor pressure osmometer and performed in triplicate at 33ºC, equivalent to the ocular surface temperature (Purslow and Wolffsohn. 2005).

Viscosity was measured using a thermostatically controlled rheometer. Viscosity was measured when the steady state was reached with shear rates increasing from 0 to 1000 s^{-1}. All determinations were made in triplicate at 33ºC.

206 *2.4. Culture conditions and liposomal formulation exposure*

207 The HCE cell line (Araki-Sasaki et al. 1995) was cultured in DMEM/F12 medium
208 supplemented with 10% fetal bovine serum, 5,000 U/mL penicillin/streptomycin, 10
209 ng/mL human epidermal growth factor, and 5 µg/mL insulin. Cells from passages 32 to
210 38 were used.

211 Cells were grown until confluence and washed in supplement-free culture medium.
212 Then, the LP formulations were diluted in supplement-free culture medium to get a final
213 PC concentration of 5 mg/mL and added to the cultured cells for 60 min. A MPA-
214 commercial formulation was used as anti-inflammatory non-LP reference formulation
215 (Medrivas®), and unexposed cells or cells exposed to the dispersion solution and blank
216 LP formulation were used as controls. After the exposure period, the cells were washed
217 3 times in phosphate buffered saline (PBS) and fresh serum-free culture medium was
218 added.

219

220 *2.5. Cytotoxicity assay*

221 To measure potential formulation toxicity, the XTT (2,3-bis-(2-methoxy-4-nitro-5-
222 sulfophenyl)-2H-tetrazolium-5-carboxanilide) cytotoxicity assay was used. After the
223 exposure period, the XTT reagent was added according to manufacturer´s instructions
224 and absorbance read. At least 3 independent experiments in triplicates were
225 performed. Benzalkonium chloride (BAC) at 0.001% was used as positive cytotoxicity
226 control. The percentage of viable cells relative to control cells was determined.

227

228 *2.6. Liposomal formulation uptake by HCE cells and localization in ex vivo porcine*
229 *corneas*

230 The C6-LP was quantified and localized by fluorometry and fluorescence
231 microscopy, respectively. To ensure that the fluorescence originated from C6-LP, a C6
232 suspension was used as the control. For fluorometry determinations, HCE cells were
233 plated in black 96-well plate and exposed to C6-LP or C6 suspension (not in
234 liposomes) for 60 min. Then, cells were washed with PBS until the fluorescent signal of
235 the PBS used for washing cells was the same that fresh PBS. The fluorescent signal
236 (excitation wavelength: 490 nm; emission wavelength: 520 nm) of the bottom of each

well was measured at 0, 24, 48, and 72 h after the exposure period. Unlabeled LP formulation in PBS was used as a blank. For fluorescence microscopy, HCE cells were plated in multichambered coverslip and exposed to C6-LP or C6 suspension for 60 min and over washed. Representative micrographs were taken at each time point using same optimized exposure time, gain, and intensity of the camera. Also, cell uptake was further characterized immediately after the exposure period. Cell nuclei were counterstained with Hoechst dye and vertical spatial images were generated by Z-scans. At least 3 independent experiments in triplicates were performed.

In addition, *ex vivo* porcine corneas were used to localize the LP formulation in the stratified corneal epithelium and stroma. Porcine eyeballs (n = 3), obtained from a local slaughterhouse, were washed with povidone iodine solution and PBS. Then, a 12-mm diameter silicon ring was placed on the central cornea, and a C6-LP or C6 suspension (not in liposomes) was applied for 5 and 60 min. Unlabeled blank LP formulation at the same exposure period was used as control. After the exposure, the eyeballs were washed with PBS and placed in 2.5% buffered paraformaldehyde. The central cornea was isolated and embedded in optimal cutting temperature compound and frozen. Representative micrographs of cryostat sections (5 µm) were taken using the same optimized exposure time, gain, and intensity for each group of samples. At least 3 independent experiments were performed.

2.7. Protein expression analysis by electrophoresis and Western blotting

Cells were homogenized in ice-cold radioimmunoprecipitation assay buffer plus protease inhibitors, and the protein content was quantified. Total protein was heated at 100˚C, and 15 µg of protein from each sample was separated by sodium dodecyl sulfate-polyacrylamide gel electrophoresis. Proteins were subsequently transferred to nitrocellulose membranes, and incubated with a blocking solution composed of tris-buffered saline containing 0.05% Tween-20, 5% powdered milk, and 2.5% bovine serum albumin for 60 min. The membranes were incubated with 2.5 µg/mL of primary antibodies in blocking solution overnight at 4°C and with peroxidase-conjugated secondary antibodies for 60 min. Receptor protein expression was normalized to GAPDH expression. At least 3 independent experiments in duplicates were performed.

2.8. Glucocorticoid receptor and progesterone receptor localization by immunofluorescence analysis

Some HCE cultures were fixed in ice-cold methanol immediately after exposure to the liposomal formulations and kept at -20˚C while others were fixed 24 h after LP exposure. Slides were washed in PBS and incubated with 0.3% Triton X-100 for 10 min. The slides were incubated at room temperature for 60 min in PBS with 4% donkey serum. They were then incubated with 5 µg/mL of primary antibodies against glucocorticoid and progesterone receptors overnight at 4°C. Alexa Fluor 488-conjugated secondary antibody was incubated for 60 min at room temperature. Cell nuclei were counterstained with propidium iodide. Negative controls omitted the primary antibodies (isotype control). Micrographs were taken using the same optimized exposure time, gain, and intensity of the camera. To calculate percentage of nuclear receptor fluorescence, green (receptor) and red (nuclei) channels were thresholded. The percentage of nuclear translocation was calculated using the following formula:

$$\%\ \text{nuclear fluorescence} = \frac{\text{receptor fluorescence localized in nuclear area}}{\text{total receptor fluorescence}}\, x\ 100$$

Where the receptor fluorescence (green) localized in the nuclear area (demarcated by red) were the mean grey value of the thresholded green channel under the thresholded red channel and the total receptor fluorescence was the mean grey value of the thresholded green channel. The values were obtained from 4 independent experiments.

2.9. Cell proliferation assay

To determine possible changes in cell proliferation rate by MPA-LP exposure, the alamarBlue® cell proliferation assay was performed at 24, 48, and 72 h after the exposure period. Fluorescence was read according to manufacturer´s instructions. At least 3 independent experiments in duplicates were performed. The percentage of proliferation in treated cultures compared with values for untreated control cells at 24 h was determined.

2.10. In vitro inflammation model

To determine if MPA-LP induced an anti-inflammatory response in HCE cells, an *in vitro* inflammation model was used as previously described (Enriquez-de-Salamanca et al. 2008). Briefly, HCE cells were stimulated with 25 ng/mL TNFα for 24 h after a washing period with supplement-free culture medium. The cells were then exposed to blank LP, MPA-LP, and the reference formulation (Medrivas®). The cells were washed with PBS and fresh medium was added. Cell supernatants were collected 48 h after the exposure period, and IL-6 and IL-8 production quantified with human IL-6 and IL-8 ELISA kits according to manufacturer´s instructions. At least 3 independent experiments in duplicates were performed. The ratio of each interleukin concentration to number of cells was calculated by the alamarBlue® assay.

2.11. Statistical Analyses

Data were expressed as means ± standard errors of the mean (SEM). Student´s *t*-test was used to compare two groups. For groups with significantly different variances (F-test), Welch´s correction was done. For more than 2 groups, we performed either a one-way analysis of variance followed by pairwise comparisons (Tukey´s test) or a Brown-Forsythe test followed by pairwise comparisons (Games-Howell test), depending on Levene's test for homogeneity of variances. Differences were considered to be significant when $p \leq 0.05$.

3. Results

3.1. Liposomal formulation characterization and biocompatibility

MPA or C6 addition to the LP composition did not change the mean diameter of liposomes (Fig. 1A, Table 1). MPA and C6 were included in the initial lipid mixture and passively loaded into the lipid bilayer of the LPs. The encapsulation efficiency was close to 94% and 89%, respectively.

The mean diameter, pH, osmolarity, and viscosity of blank, MPA- and C6-LP is shown in Table 1. The LP-based formulations did not show statistically significant differences in pH, osmolarity, and viscosity compared with the borate-trehalose-buffered LP-free solution (data not shown).

The percentage of viable HCE cells did not differ significantly from untreated cells after 60 min of exposure with either blank, MPA-, or C6-LP (Fig. 1B). The reference formulation (Medrivas®) was well tolerated while the BAC solution caused significant cell death, as expected.

3.2. Uptake and localization of LP formulation in vitro by HCE cells and epithelial localization in ex vivo porcine corneas

The cellular fluorescent signal was significantly higher after exposure to the C6-LP than after exposure to the C6 suspension at all times of analysis (Fig. 2A). However, C6 suspension can also interact with plasmatic membranes and some fluorescence was detected after sequential cell wash. Z-axis micrographs showed that after C6-LP exposure for 60 min, the fluorescence was located not only in the cell membrane but also intracellularly (Fig. 2B).

After 5 min of C6-LP exposure, the *ex vivo* porcine corneas showed fluorescence uniformly distributed throughout the corneal epithelium (Fig. 3). In contrast, penetration of the C6 suspension was largely limited to the outermost epithelial cells. After 60 min of exposure, the corneal stroma also showed fluorescent signal. However, the C6 suspension-associated fluorescence was weaker and localized only in the outermost corneal epithelial layers, supporting the permeation of the LP formulation through the cornea. There was no fluorescent signal associated with unlabeled LP formulation at any time analyzed.

3.3. Effect of MPA-LP and reference formulation (Medrivas®) on glucocorticoid and progesterone receptor protein expression in HCE cells

Glucocorticoid and progesterone receptor protein expression did not differ immediately after exposure for 60 min (Fig. 4A). However, 24 h after exposure, progesterone receptor expression was increased after MPA-LP exposure compared with the control, blank LP-, and reference formulation-exposed cells (Fig. 4B). At that time point, glucocorticoid receptor expression was decreased in reference formulation-exposed cells compared with control ($p = 0.067$), blank LP- ($p = 0.072$), and MPA-LP-exposed cells, although only the latter reached statistical significance ($p \leq 0.05$).

3.4. Effect of MPA-LP on nuclear translocation of glucocorticoid and progesterone receptors in HCE cells

There was no measurable nuclear translocation of the glucocorticoid receptor after exposure for 60 min for any of the LP or reference formulation treatments (Fig. 5A). However, immediately after the exposure period, nuclear translocation of the progesterone receptor was higher in MPA-LP-exposed cells than in blank LP-exposed and untreated cells (Fig. 5B). Twenty-four hours after the exposure, neither the glucocorticoid receptor nor the progesterone receptor translocation to the nucleus after MPA-LP exposure was evident (data not shown).

3.5. Time-dependent effect of MPA-LP on cell proliferation of HCE cells

At 24 h after the exposure period, cell proliferation in MPA-LP-exposed cells was significantly decreased compared with untreated control cells. At 48 h, the proliferation of MPA-LP-exposed cells was significantly lower than in blank LP-exposed cells (Fig. 6). Differences in cell proliferation disappeared 72 h after the exposure period.

3.6. Effect of MPA-LP on IL-6 and IL-8 production by inflamed HCE cells

Prior to determining the anti-inflammatory effect of MPA-LP, changes in glucocorticoid and progesterone receptors after TNFα stimulation were analyzed by electrophoresis and Western blotting, and immunofluorescence. Cells stimulated with TNFα did not show changes in protein expression or translocation of glucocorticoid and progesterone receptors compared with unstimulated cells (data not shown).

In response to TNFα stimulation for 24 h, the HCE cells increased IL-6 but not IL-8 production 48 h after inflammatory stimulus removal. MPA-LP exposure significantly reduced both basal and TNFα-induced IL-6 production, reaching unstimulated control levels (Fig. 7A). The reference formulation (Medrivas®) also reduced IL-6 production in basal and TNFα-stimulated cells. MPA-LP exposure also significantly reduced IL-8 production compared with the blank LP and reference formulations in TNFα-stimulated

HCE cells (Fig. 7B). Interestingly, blank LP formulation reduced IL-8 production more than did the reference formulation.

4. Discussion

In this work we report that a LP formulation, loaded with an anti-inflammatory drug, efficiently permeated through corneal epithelial barriers, activated specific drug receptors, and reduced the production of inflammatory cytokines IL-6 and IL-8 in cultured HCE cells. The scarcity of anti-inflammatory drugs in the market drove us to include an anti-inflammatory agent in a LP formulation designed as artificial tears to treat DED (Vicario-de-la-Torre et al. 2014). We selected the anti-inflammatory hormone MPA whose properties make it a good steroid-sparing agent, often used to decrease the dependency of a long-term therapy with steroids in ocular surface inflammatory diseases.

Taking into account the special requirements for topical ophthalmic formulations, i.e., pH = 6-9, osmolarity = 150-320 mOsm, viscosity < 20 mPas (Ali and Lehmussaari. 2006, Ammar et al. 2009), the values of our LP-based formulations (Table 1) met all the requirements to be used as eyedrops. The liposomal formulation was comprised of components not only similar to those present in the natural tears, such as PC and cholesterol, but also antioxidants (vitamin E) and molecules able to provide special benefits for the ocular surface (trehalose) (Li et al. 2012, Pinto-Bonilla et al. 2015). Also, our liposomal formulation does not contain any preservative, thus avoiding the well-known harmful side effects associated with them (Baudouin et al. 2010).

We labeled the LP formulation with C6 to localize it in HCE cells and in ex vivo corneas after 5 and 60 min of exposure. Although the encapsulation efficiency for C6 was always around 90%, free C6 can penetrate through cell membranes. Consequently, we used a C6 suspension as control to distinguish LP-associated fluorescence from that caused by C6 in suspension. How the LPs bind to and are endocytosed by cultured cells has been widely reviewed (Duzgune&scedil et al. 1999, Lee et al. 1993). LP composition, charge, and size, as well as the types of cells to which they are exposed, influence the cellular uptake. Therefore, we analyzed cellular uptake of the LP formulation by HCE cells. It is important to point out that serum was avoided in all experiments as it partly inhibits the uptake of LPs (Duzgune&scedil et al. 1999). Results showed LP-associated fluorescence in HCE cells immediately, 24, 48,

and 72 h after 60 min of exposure. Immediately after the exposure period, the cells had nanometer-sized dots, indicating that the LP did not aggregate in the formulation. Moreover, these dots corresponding to LPs are within the cell membranes and in the cytosol, as determined by Z-axis micrographs. This documents the efficient interaction of the LPs with the cultured cells and confirmed fast uptake by HCE cells in vitro.

To mimic actual *in vivo* exposure times, C6-LP was in contact with corneal tissues for only 5 min (Davies. 2000). After C6-LP exposure, the corneas showed fluorescence through the stratified epithelium, including the basal layers. After 60 min of C6-LP exposure, the corneal stroma was also stained. We therefore demonstrated that LP formulation was taken up by all epithelial layers and reached the corneal stroma after longer exposure times.

MPA binds to progesterone, glucocorticoid, androgen, mineralocorticoid, and estrogen receptors (Sitruk-Ware. 2004). For this study, we analyzed changes in protein expression and nuclear translocation of the glucocorticoid and progesterone receptors, which have greater affinity for the drug (Sitruk-Ware. 2004). Glucocorticoid and progesterone receptors are closely related members of the steroid receptor family, which act as ligand-activated transcription factors with well-characterized mechanisms of action. After binding a specific ligand, the receptors dimerize, and the dimers are then translocated to the nucleus, allowing the ligand-receptor complex to target specific DNA sequences (hormone response elements), affecting the inflammatory signaling cascade (Mangelsdorf et al. 1995). We calculated the percentage of glucocorticoid and progesterone receptors translocated to the nucleus in immunofluorescence micrographs as an indicator of receptor activation. Our results showed that while changes in nuclear translocation were observed immediately after the exposure time, the protein expression did not change at this time point and the effect of the drug was observed after 24 h of the exposure time. The progesterone receptor was activated after MPA-LP exposure, suggesting that MPA was released into cells. The translocation and the increased expression of the progesterone receptor, but not the glucocorticoid receptor, after MPA-LP exposure agrees with a study reporting a higher affinity of MPA for the progesterone receptor than for the glucocorticoid receptor (Sitruk-Ware. 2004). Unexpectedly, the protein expression of glucocorticoid receptor was decreased 24 h after reference formulation exposure. This effect may be due to the vasoconstrictor or the different excipients included in this formulation which interacts with the glucocorticoid receptor and can modify the expression of this receptor. It also could explain the lesser effect observed in proliferation or inflammation

experiments. However, the analysis of the effect caused by those excipients is out of the scope of this study and more experiments need to be done to clarify this effect.

Corticosteroids affect *in vitro* cell proliferation; therefore, we analyzed changes in HCE cell proliferation using a standard proliferation assay. In previous studies, MPA reduced breast cancer epithelial cell proliferation (Cops et al. 2008, Sutherland et al. 1988), but did not affect corneal fibroblast proliferation (Zhou et al. 2012). Our findings showed a decrease in the proliferation rate of HCE cells 48 h after MPA exposure, which further supports efficient MPA transport by the LP formulation to the cells.

To determine the anti-inflammatory effect of MPA-LP in terms of reduction of IL-6 and/or IL-8 production, we optimized a cytokine-induced inflammation model using HCE cells. TNFα was used as an inflammatory stimulus, and the cytokine IL-6 and the chemokine IL-8 were used as inflammatory markers. The production of both inflammatory markers increased after TNFα stimulation in conjunctival epithelial cell line (Enriquez-de-Salamanca et al. 2008), and both are increased in the tears of patients with inflammatory diseases (Lam et al. 2009, Massingale et al. 2009). The production of both cytokines was analyzed 48 h after the exposure of TNFα. This time point was chosen because changes in the cell proliferation rate emerged 48 h after the MPA-LP exposure period, with C6-LP-associated fluorescence in the cells. Furthermore, a previous report using corneal fibroblasts showed MPA-induced collagen degradation after 36 h of exposure period (Zhou et al. 2012). To rule out a pro-inflammatory effect induced by components of the liposomal formulation (Joffre et al. 2007, Rodriguez and Larrayoz. 2010), blank LP formulation with different cholesterol concentrations were tested, and no inflammation-associated effects were present (data not shown). According to our data, the exposure of MPA-LP and the reference formulation (Medrivas®) reduced IL-6 production by HCE cells. However, only MPA-LP reduced IL-8 production. Interestingly, blank LP formulation also reduced IL-8 production in comparison to the reference formulation-treated cells and control cells, although the latter did not reach significance. This result confirms the importance of a vehicle in drug administration, not only to protect the drug and increase the residence time in the ocular surface, but also to enhance therapeutic effect of the drug. This is in agreement with previous data reporting that components of the blank LP formulation, such as PC, trehalose, and vitamin E down-regulate IL-8 production of different epithelial cells in vitro (Cejkova et al. 2011, Ekstrand-Hammarstrom et al. 2007, Elisia and Kitts. 2015, Treede et al. 2009).

Although the *in vitro* and *ex vivo* results obtained with MPA-LP are promising, only *in vivo* experiments can evaluate the effect of physiological mechanisms such as the stress generated by eyelid wiping and tear flow on the liposomal formulation. In addition, the reference formulation (Medrivas®) contains not only the preservative BAC but also a vasoconstrictor, tetryzoline chlorhydrate, which might have effects that could not be assessed with our current *in vitro* approach.

5. Conclusions

To conclude, our findings show that an anti-inflammatory agent such as MPA loaded in the LP formulation permeated *ex vivo* through corneal barriers and was efficiently delivered to corneal epithelial cells. Also, the delivered MPA *in vitro* activated specific drug receptors and showed anti-proliferative and anti-inflammatory effects in HCE cells. Consequently, when applied topically as eyedrops, MPA-LP may attach to the hydrophobic corneal epithelium and continuously release the encapsulated drug, improving its biodistribution. In addition, the liposomal formulation does not contain preservatives or other bioactive agents required in the reference formulation, thus avoiding harmful side effects. In this sense, anti-inflammatory drugs included in unpreserved artificial tears can be useful for the treatment of inflammatory processes associated with DED or other ocular surface disorders that involve any inflammatory surface reactions.

Acknowledgements

The authors acknowledge the assistance of Britt Bromberg, PhD, ELS, of Xenofile Editing (http://www.xenofileediting.com) for the final editing and preparation of this manuscript.

This work was supported by Spanish Ministry of Economy and Competitiveness (FEDER-CICYT MAT2013-47501-CO2-1-R); Regional Junta de Castilla y León Scholarship/European Social Fund Program (VA098-12); Complutense University of Madrid (920415 GR/14); and Spanish Ministry of Health (RETICS-RD07/0062/0013, FEDER-CICYT FIS-PI10/00645 and FIS-PI10/00993).

521 **References**

522 Ali Y., Lehmussaari K., 2006. Industrial perspective in ocular drug delivery. Adv. Drug
523 Deliv. Rev. 58, 1258-1268.

524 Ammar H.O., Salama H.A., Ghorab M., Mahmoud A.A., 2009. Nanoemulsion as a
525 potential ophthalmic delivery system for dorzolamide hydrochloride. AAPS
526 PharmSciTech 10, 808-819.

527 Araki-Sasaki K., Ohashi Y., Sasabe T., Hayashi K., Watanabe H., Tano Y., Handa H.,
528 1995. An SV40-immortalized human corneal epithelial cell line and its characterization.
529 Invest. Ophthalmol. Vis. Sci. 36, 614-621.

530 Baudouin C., Labbe A., Liang H., Pauly A., Brignole-Baudouin F., 2010. Preservatives
531 in eyedrops: the good, the bad and the ugly. Prog. Retin. Eye Res. 29, 312-334.

532 Cejkova J., Ardan T., Cejka C., Luyckx J., 2011. Favorable effects of trehalose on the
533 development of UVB-mediated antioxidant/pro-oxidant imbalance in the corneal
534 epithelium, proinflammatory cytokine and matrix metalloproteinase induction, and heat
535 shock protein 70 expression. Graefes Arch. Clin. Exp. Ophthalmol. 249, 1185-1194.

536 Cops E.J., Bianco-Miotto T., Moore N.L., Clarke C.L., Birrell S.N., Butler L.M., Tilley
537 W.D., 2008. Antiproliferative actions of the synthetic androgen, mibolerone, in breast
538 cancer cells are mediated by both androgen and progesterone receptors. J. Steroid
539 Biochem. Mol. Biol. 110, 236-243.

540 Davies N.M., 2000. Biopharmaceutical considerations in topical ocular drug delivery.
541 Clin. Exp. Pharmacol. Physiol. 27, 558-562.

542 Di Tommaso C., Bourges J.L., Valamanesh F., Trubitsyn G., Torriglia A., Jeanny J.C.,
543 Behar-Cohen F., Gurny R., Moller M., 2012. Novel micelle carriers for cyclosporin A
544 topical ocular delivery: in vivo cornea penetration, ocular distribution and efficacy
545 studies. Eur. J. Pharm. Biopharm. 81, 257-264.

546 Diebold Y., Calonge M., 2010. Applications of nanoparticles in ophthalmology. Prog.
547 Retin. Eye Res. 29, 596-609.

548 Duzgune&scedil, N., Nir S., 1999. Mechanisms and kinetics of liposome-cell
549 interactions. Adv. Drug Deliv. Rev. 40, 3-18.

550 Ekstrand-Hammarstrom B., Osterlund C., Lilliehook B., Bucht A., 2007. Vitamin E
551 down-modulates mitogen-activated protein kinases, nuclear factor-kappaB and
552 inflammatory responses in lung epithelial cells. Clin. Exp. Immunol. 147, 359-369.

553 Elisia I., Kitts D.D., 2015. Tocopherol isoforms (alpha-, gamma-, and delta-) show
554 distinct capacities to control Nrf-2 and NfkappaB signaling pathways that modulate
555 inflammatory response in Caco-2 intestinal cells. Mol. Cell. Biochem. 404, 123-131.

556 Enriquez-de-Salamanca A., Calder V., Gao J., Galatowicz G., Garcia-Vazquez C.,
557 Fernandez I., Stern M.E., Diebold Y., Calonge M., 2008. Cytokine responses by
558 conjunctival epithelial cells: an in vitro model of ocular inflammation. Cytokine 44, 160-
559 167.

560 Hathout R.M., Mansour S., Mortada N.D., Guinedi A.S., 2007. Liposomes as an ocular
561 delivery system for acetazolamide: in vitro and in vivo studies. AAPS PharmSciTech 8,
562 1.

563 Joffre C., Leclere L., Buteau B., Martine L., Cabaret S., Malvitte L., Acar N., Lizard G.,
564 Bron A., Creuzot-Garcher C., Bretillon L., 2007. Oxysterols induced inflammation and
565 oxidation in primary porcine retinal pigment epithelial cells. Curr. Eye Res. 32, 271-280.

566 Lam H., Bleiden L., de Paiva C.S., Farley W., Stern M.E., Pflugfelder S.C., 2009. Tear
567 cytokine profiles in dysfunctional tear syndrome. Am. J. Ophthalmol. 147, 198-205. e1.

568 Law S.L., Huang K.J., Chiang C.H., 2000. Acyclovir-containing liposomes for potential
569 ocular delivery. Corneal penetration and absorption. J. Control. Release 63, 135-140.

570 Lee K.D., Nir S., Papahadjopoulos D., 1993. Quantitative analysis of liposome-cell
571 interactions in vitro: rate constants of binding and endocytosis with suspension and
572 adherent J774 cells and human monocytes. Biochemistry 32, 889-899.

573 Li J., Roubeix C., Wang Y., Shi S., Liu G., Baudouin C., Chen W., 2012. Therapeutic
574 efficacy of trehalose eye drops for treatment of murine dry eye induced by an
575 intelligently controlled environmental system. Mol. Vis. 18, 317-329.

576 Lim A., Wenk M.R., Tong L., 2015. Lipid-Based Therapy for Ocular Surface
577 Inflammation and Disease. Trends Mol. Med. .

578 Mangelsdorf D.J., Thummel C., Beato M., Herrlich P., Schutz G., Umesono K.,
579 Blumberg B., Kastner P., Mark M., Chambon P., Evans R.M., 1995. The nuclear
580 receptor superfamily: the second decade. Cell 83, 835-839.

581 Massingale M.L., Li X., Vallabhajosyula M., Chen D., Wei Y., Asbell P.A., 2009.
582 Analysis of inflammatory cytokines in the tears of dry eye patients. Cornea 28, 1023-
583 1027.

584 Patel A., Cholkar K., Agrahari V., Mitra A.K., 2013. Ocular drug delivery systems: An
585 overview. World J. Pharmacol. 2, 47-64.

586 Pflugfelder S.C., Solomon A., Stern M.E., 2000. The diagnosis and management of dry
587 eye: a twenty-five-year review. Cornea 19, 644-649.

588 Pinto-Bonilla J.C., Del Olmo-Jimeno A., Llovet-Osuna F., Hernandez-Galilea E., 2015.
589 A randomized crossover study comparing trehalose/hyaluronate eyedrops and

590 standard treatment: patient satisfaction in the treatment of dry eye syndrome. Ther.
591 Clin. Risk Manag. 11, 595-603.

592 Purslow C., Wolffsohn J.S., 2005. Ocular surface temperature: a review. Eye Contact
593 Lens 31, 117-123.

594 Rodriguez I.R., Larrayoz I.M., 2010. Cholesterol oxidation in the retina: implications of
595 7KCh formation in chronic inflammation and age-related macular degeneration. J. Lipid
596 Res. 51, 2847-2862.

597 Schaeffer H.E., Krohn D.L., 1982. Liposomes in topical drug delivery. Invest.
598 Ophthalmol. Vis. Sci. 22, 220-227.

599 Shabir G.A., 2003. Validation of high-performance liquid chromatography methods for
600 pharmaceutical analysis. Understanding the differences and similarities between
601 validation requirements of the US Food and Drug Administration, the US
602 Pharmacopeia and the International Conference on Harmonization. J. Chromatogr. A
603 987, 57-66.

604 Sitruk-Ware R., 2004. Pharmacological profile of progestins. Maturitas 47, 277-283.

605 Sutherland R.L., Hall R.E., Pang G.Y., Musgrove E.A., Clarke C.L., 1988. Effect of
606 medroxyprogesterone acetate on proliferation and cell cycle kinetics of human
607 mammary carcinoma cells. Cancer Res. 48, 5084-5091.

608 Treede I., Braun A., Jeliaskova P., Giese T., Fullekrug J., Griffiths G., Stremmel W.,
609 Ehehalt R., 2009. TNF-alpha-induced up-regulation of pro-inflammatory cytokines is
610 reduced by phosphatidylcholine in intestinal epithelial cells. BMC Gastroenterol. 9, 53-
611 230X-9-53.

612 Vicario-de-la-Torre M., Benitez-del-Castillo J.M., Vico E., Guzman M., de-Las-Heras B.,
613 Herrero-Vanrell R., Molina-Martinez I.T., 2014. Design and characterization of an
614 ocular topical liposomal preparation to replenish the lipids of the tear film. Invest.
615 Ophthalmol. Vis. Sci. 55, 7839-7847.

616 Zhou H., Kimura K., Orita T., Nishida T., Sonoda K.H., 2012. Inhibition by
617 medroxyprogesterone acetate of interleukin-1beta-induced collagen degradation by
618 corneal fibroblasts. Invest. Ophthalmol. Vis. Sci. 53, 4213-4219.

619

620

621 **Figure legends**

622 Figure 1: **Diameter size distribution and cytotoxicity**. (A) The diameter size
623 distribution of the liposomal formulation did not change with the addition of MPA or C6
624 as determined by dynamic light scattering. (B) The percentage of viable cells did not
625 differ from untreated cells with either blank, MPA- or C6- LP formulations after 60 min
626 of exposure in HCE cells as measured by the XTT assay. ***$P \leq 0.001$ compared with
627 control. LP: liposome-based formulation; C6-LP: liposome-based formulation loaded
628 with coumarin-6; MPA-LP: liposome-based formulation loaded with
629 medroxyprogesterone acetate; BAC: benzalkonium chloride.

630 Figure 2: **Uptake and distribution in human corneal epithelial cells**. (A) At all times
631 analyzed, the cellular fluorescent signal was significantly higher after C6-LP exposure
632 than after C6 suspension exposure in HCE cells as determined by fluorescence
633 microscopy (left) and fluorometry (right). (B) After the exposure time, C6-LP was taken
634 up by HCE cells as Z-scans showed intracellular C6-LP localization. C6 stained in
635 *green* and nuclei were stained in *blue* with Hoechst dye. **$P \leq 0.01$; *** $P \leq 0.001$,
636 compared at same time points. LP: liposome-based formulation; C6: coumarin-6; C6-
637 LP: liposome-based formulation loaded with C6. Scale bar: 50 µm.

638 Figure 3: **Localization in *ex vivo* porcine corneas**. C6-LP was uniformly distributed
639 throughout the corneal epithelium in *ex vivo* corneas after 5 min and 60 min of
640 exposure. Arrows show stromal localization of C6-LP after 60 min of exposure in *ex*
641 *vivo* porcine corneas. LP: liposome-based formulation; C6: coumarin-6; C6-LP:
642 liposome-based formulation loaded with C6. Scale bar: 50 µm.

643 Figure 4: **Changes in the expression of glucocorticoid and progesterone**
644 **receptors in human corneal epithelial cells**. Although no changes were shown
645 immediately after (T 0 h) the exposure period (A), MPA-LP-exposed cells increased
646 progesterone receptor expression compared with control, blank LP, and reference
647 formulation-exposed cells after 24 h (T 24 h) the exposure period (B), as determined by
648 electrophoresis and Western blotting. *$P \leq 0.05$; **$P \leq 0.01$. LP: liposome-based
649 formulation; MPA-LP: liposome-based formulation loaded with medroxyprogesterone
650 acetate; GR: glucocorticoid receptor; PR: progesterone receptor; Rs: receptors;
651 GAPDH: glyceraldehyde 3-phosphate dehydrogenase.

652 Figure 5: **Nuclear translocation (activation) of glucocorticoid and progesterone**
653 **receptors in human corneal epithelial cells.** Although no changes were shown in
654 glucocorticoid receptor nuclear translocation (A), MPA-LP-exposed cells increased

nuclear translocation of progesterone receptor compared with control and blank LP-exposed cells (B) determined by fluorescence microscopy. Receptors stained in *green* and nuclei were stained in *red* with propidium iodide. Graph shows the percentage of nuclear receptor fluorescence calculated by measuring the receptor staining in the nuclear area to the total receptor staining. *$P \leq 0.05$. LP: liposome-based formulation; MPA-LP: liposome-based formulation loaded with medroxyprogesterone acetate; GR: glucocorticoid receptor; PR: progesterone receptor; Iso Con: isotype controls including omission of primary antibodies. Scale bar: 50 μm.

Figure 6: **Changes in corneal epithelial cell proliferation**. MPA-LP-exposed cells reduced cell proliferation compared with blank LP-exposed cells 48 h after the exposure period as determined by the alamarBlue® assay. *$P \leq 0.05$, compared with control, if not otherwise indicated by straddle bars. LP: liposome-based formulation; MPA-LP: liposome-based formulation loaded with medroxyprogesterone acetate.

Figure 7: **Changes in inflammatory cytokine production in inflamed human corneal epithelial cells**. MPA-LP-exposed cells reduced IL-6 and IL-8 production compared with control and blank LP-exposed cells 48 h after the exposure period as determined by ELISA. Note the difference in scales for the y-axes of panels A and B. *$P \leq 0.05$; **$P \leq 0.01$; ***$P \leq 0.001$, compared with control, if not otherwise indicated by straddle bars. LP: liposome-based formulation; MPA-LP: liposome-based formulation loaded with medroxyprogesterone acetate; IL: interleukin; TNFα: tumor necrosis factor-alpha.

Table 1: Liposomal formulation diameter, pH, osmolarity, and viscosity.

	Blank LP	MPA-LP	C6-LP
Diameter (nm)	191.6 ± 2.4	185.5 ± 3.5	188.1 ± 2.0
pH	7.4 ± 0.1	7.4 ± 0.2	7.5 ± 0.3
Osmolarity (mOsm)	202.4 ± 0.1	206.0 ± 0.2	206.7 ± 0.3
Viscosity (mPas)	3.1 ± 1.1	3.0 ± 0.6	3.1 ± 1.0

LP: liposome-based formulation; C6: coumarin-6; MPA-LP: liposome-based formulation loaded with medroxyprogesterone acetate; C6-LP: liposome-based formulation loaded with C6.

1A

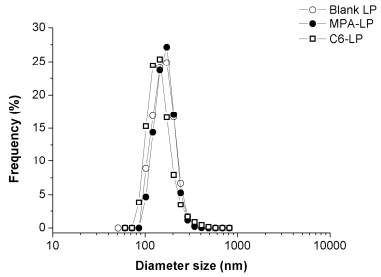

1B

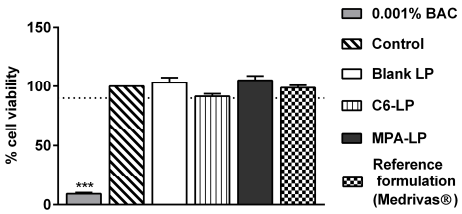

2A

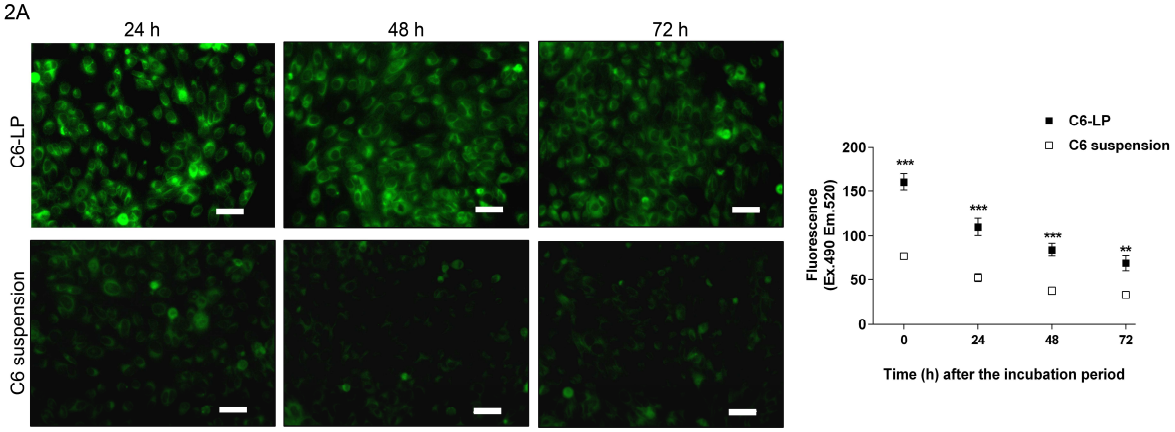

2B

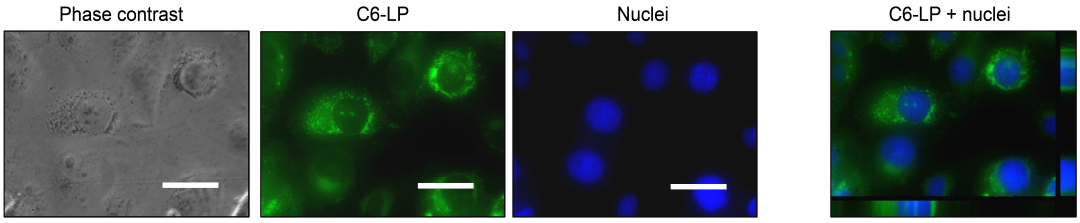

3

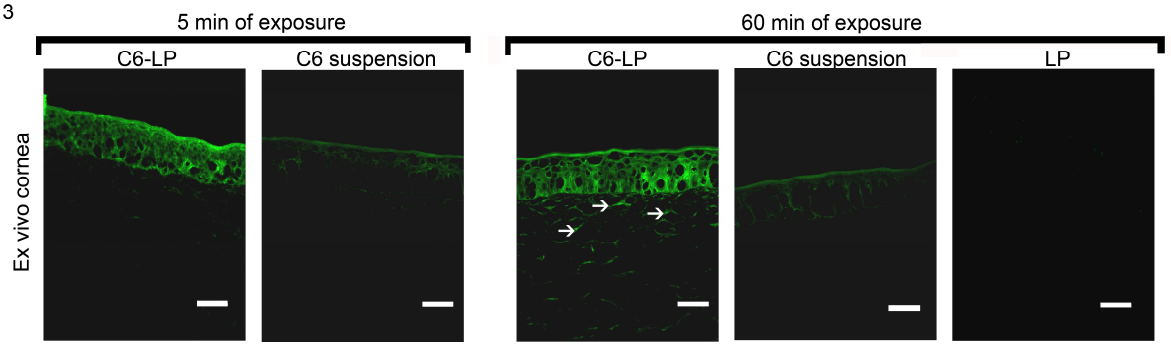

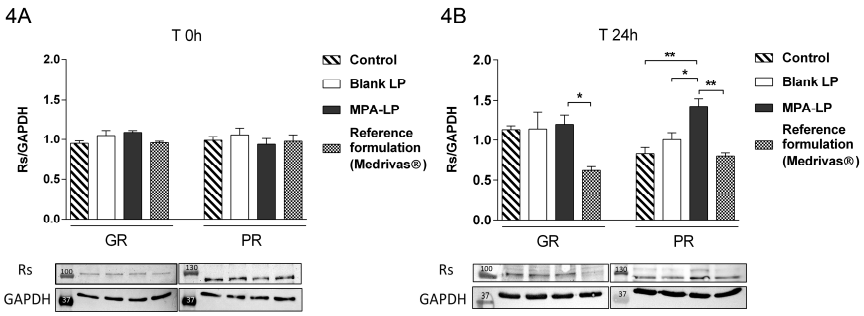

5A

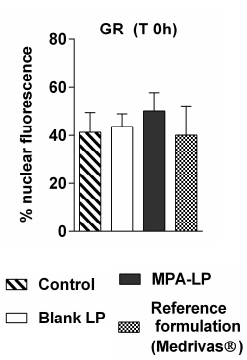

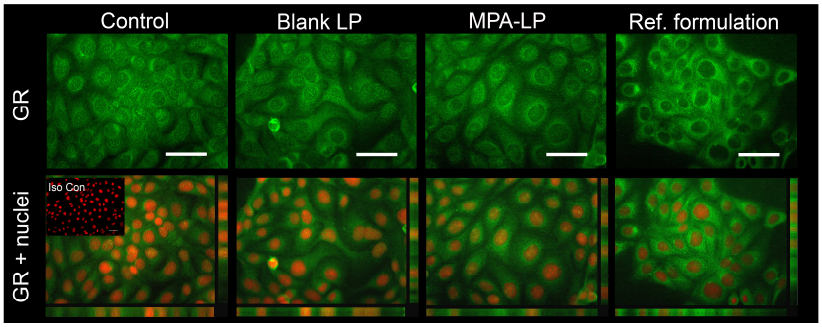

5B

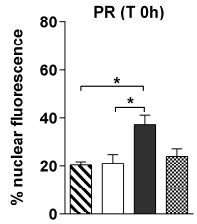

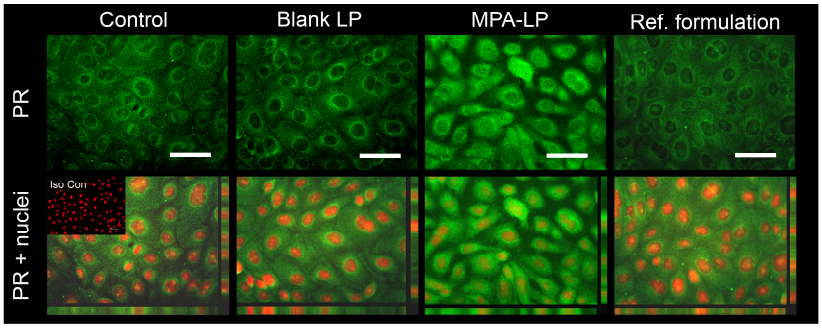

6

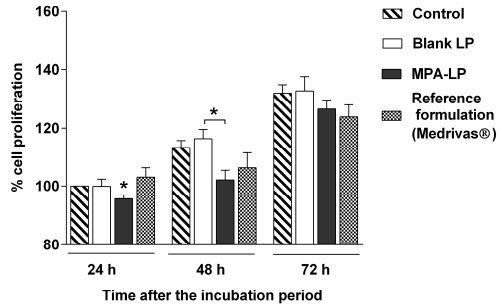

7A

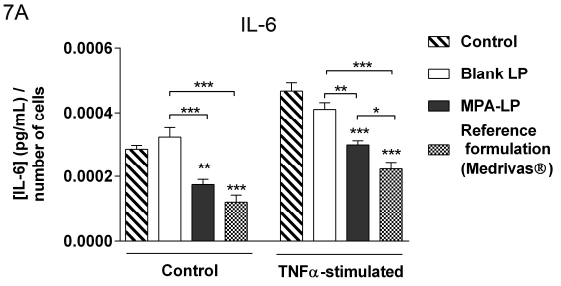

7B

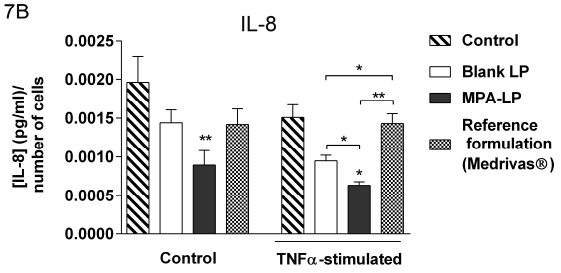

HIGHLIGHTS

- Medroxyprogesterone was incorporated into a liposomal artificial tear formulation.
- Encapsulated drug readily penetrates corneal tissue in an ex vivo porcine model.
- Encapsulated drug exerts anti-inflammatory effects in human corneal cells in vitro.
- The novel liposomal artificial tears enhance the effect of the drug in vitro.